Design and Fabrication of a Narrow-Bandwidth Micromechanical Ring Filter using a Novel Process in UV-LIGA Technology

A. Bijari*, S. H. Keshmiri*, W. Wanburee**, C. Sriphung***, R. Phatthanakun***

Abstract: This paper presents a novel low-cost fabrication process for micromechanical filter in UV-LIGA technology. The micromechanical filter consists of the two identical bulk-mode ring resonators, mechanically coupled by a flexural-mode beam. The design procedure is performed by a mechanical lumped element model and ANSYS software. The low-cost fabrication process with only three UV-lithography steps is used to achieve a high aspect ratio of 20 with 3 μm gap spacing. The fabricated filter is characterized using a fully differential drive and sense interface circuit. The experimental results demonstrates micromechanical filter with a center frequency of 10.31 MHz and percent bandwidth less than 0.3% using a DC-bias voltage of 60 V. The detailed fabrication process can be applied as an appropriate alternative to X-ray LIGA and silicon-based micromechanical filters.

Keywords: Micromechanical Ring Filter, Nickel Electroplating, SU-8 Photoresist, UV-LIGA.

1 Introduction

Micromechanical devices are currently the key components in micro-communication applications [1]. Band-pass filters with narrow-bandwidth, low insertion loss and excellent stop-band rejection, are essential parts of newly-invented radio frequency (RF) channel-select transceiver architecture [2, 3]. Due to compatibility with IC technologies and small size, micromechanical filters can potentially serve as direct on-chip replacements for their off-chip crystal and surface acoustic wave (SAW) filters in wireless transceivers [4]. Today, how to develop micromechanical filter with new material and low-cost fabrication process is a matter of debate. There are several technologies for fabricating micromechanical resonators and filters such as LIGA (a German acronym for Lithographie, Galvanoformung, Abformung), surface and bulk micromachining. Bannon et al [5] used a polysilicon surface micromachining process to fabricate a micromechanical filter, which was composed of two clamped–clamped beam resonators coupled mechanically by a flexural beam. The filter had a center frequency of 7.81 MHz, with a 0.23% bandwidth, and an insertion loss less than 2 dB. Motiee et al [6] utilized Poly MUMPs process to fabricate mechanical coupled filter, with a center frequencies of 1.7 MHz, using as a novel V-shape beam coupler. The V-shape architecture was reported to improve the filter performance and flatten the response in the passband. Abdolvand et al [7] presented an implementation of a narrow-bandwidth filter with a center frequency of 800 kHz and a percent bandwidth of 0.02 % using the high aspect ratio process (HARPSS). Wang et al [8] demonstrated a 20 MHz narrow-bandwidth filter as small as 0.029%, using mechanically coupled breathe-mode ring resonators, and they analyzed the effect of the coupling beam width on the filter bandwidth. In the aforementioned studies, Single Crystal Silicon (SCS) and polysilicon were used as structural material. In recent years, new materials such as nickel (Ni) have developed due to their relatively low cost on the silicone substrate [9, 10]. Compared to the more conventional micro-fabrication processes based on new material, LIGA process allows the fabrication of high aspect ratio with excellent sidewall quality. This feature makes it very suitable for fabricating capacitive micromechanical resonators [11]. However, highly expensive synchrotron source and X-ray mask costs make it difficult for low-cost applications. The paper deals with a novel low-cost

Iranian Journal of Electrical & Electronic Engineering, 2012.
Paper first received 5 Aug. 2012 and in revised form 4 Nov. 2012.
* The Authors are with the Department of Electrical Engineering, Faculty of Engineering, Ferdowsi University of Mashhad (FUM), 91775-1111, Iran.
E-mails: a.bijari@gmail.com, keshmiri@um.ac.ir.
** The Author is with the School of Electrical Engineering, Institute of Engineering, Suranaree University of Technology (SUT), Nakhon Ratchasima 30000, Thailand.
*** The Authors are with the Synchrotron Light Research Institution (SLRI), Nakhon Ratchasima 30000, Thailand.

fabrication method based on UV-LIGA. Micromechanical ring filter is first designed at the center frequency of 10.7 MHz and bandwidth of 30 kHz using a mechanical lumped element model and ANSYS software. The fabrication process steps are then detailed. Finally, the fabricated filter is characterized and discussed.

2 Micromechanical Ring Filter Structure and Operation

Micromechanical ring resonators, due to their high structural stiffness, ring geometry and having four quasi-nodal points at their outer periphery in some in-plane bulk-modes, offer lower motional resistance and higher quality factors [12]. Hence, these resonators are more attractive alternative to flexural-mode resonators in filter applications. Mechanical coupling of two identical micromechanical resonators is the most common approach for implementation of the second-order filters. In the approach, bulk-mode ring resonators are mechanically coupled via compliant elements resulting in two resonance modes for the whole system. In the lower resonance mode, the ring resonators are 180 out of phase, and in the higher resonance mode, both resonators vibrate in phase as shown in Fig. 1(a). Fig. 1(b), presents a schematic view of a coupled ring filters.

As shown, the filter consists of two identical ring resonators, which are anchored by three support beams. Ring resonators are mechanically coupled by a coupling beam with stiffness of k_{cb}, at the outer ring peripheries. Two electrodes are placed at quadrants overlapping the outside of each ring resonators to drive and sense resonant vibration [4, 13]. An *ac* input signal (v_i) is applied through a properly-valued input termination resistor (R_Q), to the drive electrodes, and the structure is biased to a DC voltage (V_P).

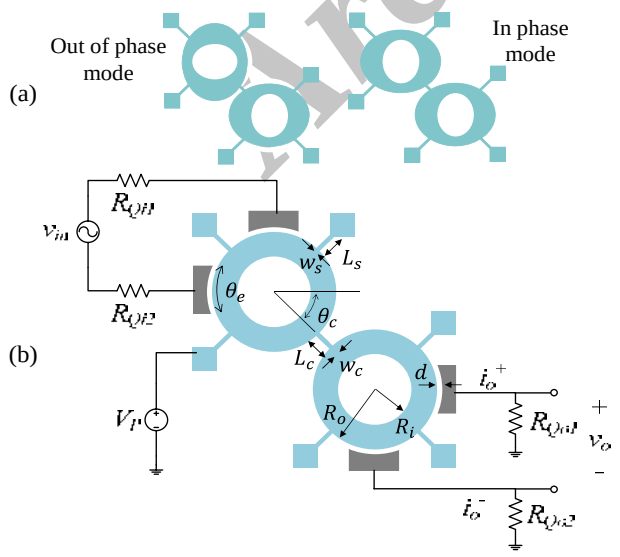

Fig. 1(a) Filter mode shapes (extensional w.-glass (EWG) mode) (b) Schematic view of the micromechanical ring filter.

This combined input generates an electrostatic force between the drive electrodes and the input resonator that induces vibration when the frequency of v_i falls within the filter pass-band. The vibration energy is passed to the center and output resonator via the coupling beam, causing it to vibrate as well. The output resonator vibrations create DC-biased, time varying capacitors between the output resonator and sense electrodes, and source motional output currents (i_o) [14]. Based on the lumped element model developed for bulk-mode ring resonator [15], the simplified lumped mass-spring model of ring filters is presented as shown in Fig. 2. Each resonator is assumed as two separate ring resonators coupled together at the middle distance between the inner and outer edges. In Fig. 2, x_i represents the vibration displacement of the effective lumped mass (M_r). The k_{rc} and k_{cr} are the resonator mechanical stiffness at the coupling location and internal coupling stiffness, respectively. The subscripts *i* and *o* denote the inner and outer ring resonators, respectively. The effective lumped mass and mechanical stiffness at the coupling location for the ring resonator are given by:

$$M_{rc} = \rho t \left[\frac{\int_{\frac{R_i+R_o}{2}}^{R_o} \int_0^{2\pi} U_r^2 \cos^2(n\theta) r dr d\theta}{U_{ro}^2 \cos^2(n\theta_c) + U_{\theta o}^2 \sin^2(n\theta_c)} + \gamma \frac{\int_{R_i}^{\frac{R_i+R_o}{2}} \int_0^{2\pi} U_r^2 \cos^2(n\theta) r dr d\theta}{U_i^2} \right] \quad (1)$$

$$k_{rc} = 4\pi^2 M_{rc} f_{nm}^2 \quad (2)$$

$$f_{nm} = \frac{h_{nm}}{2\pi} \sqrt{\frac{E}{\rho(1-\upsilon^2)}} \quad (3)$$

where, f_{nm} is the resonance frequency of the bulk-mode

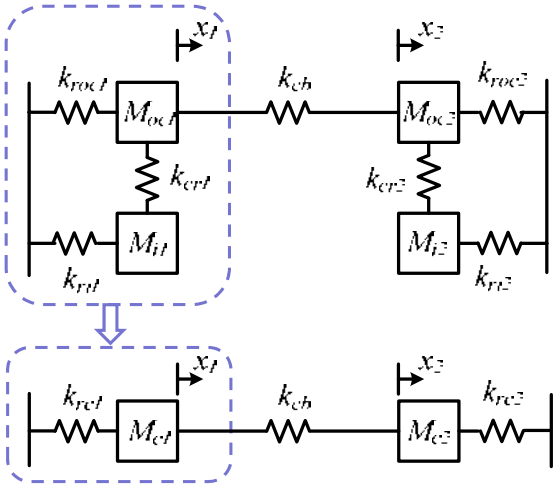

Fig. 2 The equivalent lumped mass-spring model of the micromechanical ring filter.

of (*n*,*m*), where *n* corresponds to the circumferential order and *m* corresponds to the radial harmonic. The *E*, υ and ρ are Young's modulus, Poisson's ratio and density of the structural material, respectively.

Furthermore, t and θ_c are the thickness of the ring resonators and coupling angle, respectively. The parameter $\gamma=|U_{ri}/U_{ro}|$ denotes the inner to outer radial displacement ratio, which the radial displacement (U_r) and circumferential displacement (U_θ) are expressed as follow:

$$U_r = \frac{A_n}{h_{nm}}\left[\frac{d}{dr}\left(J_n(h_{nm}r)+\frac{B_n}{A_n}Y_n(h_{nm}r)\right) + \frac{n}{r}\left(\frac{C_n}{A_n}J_n(k_{nm}r)+\frac{D_n}{A_n}Y_n(k_{nm}r)\right)\right] \quad (4)$$

$$U_\theta = -\frac{A_n}{h_{nm}}\left[\frac{n}{r}\left(J_n(h_{nm}r)+\frac{B_n}{A_n}Y_n(h_{nm}r)\right) + \frac{d}{dr}\left(\frac{C_n}{A_n}J_n(k_{nm}r)+\frac{D_n}{A_n}Y_n(k_{nm}r)\right)\right] \quad (5)$$

In the above equations, J_n and Y_n are Bessel functions of the first and second kind, respectively. The relationship between the mode consonants of k_{nm} and h_{nm} is given by: $k_{nm}/h_{nm} = \sqrt{2}/(1-\upsilon)$. The elastic wave constants of (B_n/A_n, C_n/A_n, B_n/A_n) can be found by solving the following equation of det ($\mathbf{M}_{4\times4}$) = 0, which the elements of **M** were explained in detail in [12, 16]. According to the electrostatic force applying to the two identical coupled ring resonators, the coupling beam provides the sufficient to shift the resonator frequencies, creating two close resonance modes that form the pass-band as follows:

$$f_1 = \frac{1}{2\pi}\sqrt{\frac{k_{re}}{M}} \quad , \quad f_2 = \frac{1}{2\pi}\sqrt{\frac{k_{re}+2k_{cb}}{M}} \quad (6)$$

where, k_{re} is the effective mechanical stiffness at the coupling locationdue to electrical nonlinearity, and for the ring resonator operating in their second-order bulk-modes (i.e., w.-glass (2, 1), extensional w.-glass (2, 4), etc) is given by:

$$k_{re} = k_{rc}\left[1-\frac{\varepsilon_0 t R_o V_P^2}{k_r d^3}(sin(2\theta_e)+2\theta_e)\right] \quad (7)$$

where, ε_0, θ_e and d denote the vacuum permittivity, electrode-to-resonator overlap angle and gap spacing, respectively. According to Eq. (6), the bandwidth of the micromechanical ring filter is approximately determined as follows:

$$BW = \frac{f_1}{k_{12}}\frac{k_{cb}}{k_{re}} \quad (8)$$

where, k_{12} is the normalized coupling coefficient for a given filter type.

3 Micromechanical Ring Filter Design

3.1 Coupling Beam Design

One of the main challenges in narrow-bandwidth filters is providing a small coupling stiffness (k_{cb}) between constituent resonators. Flexural-mode beam was chosen to serve as a coupling element at the outer ring periphery with the coupling angle of $\pi/4$. The beam stiffness of the coupling beam with sliding ends is given by [5]:

$$k_{cb} = -\frac{Ew_c^3 t\alpha^3(sin\,\alpha+sinh\,\alpha)}{12L_c^3(cos\,\alpha\,cosh\,\alpha-1)} \quad (9)$$

where the subscript *c* denotes the coupling beam and

$$\alpha = L_c\sqrt[4]{\frac{48\pi^2\rho f_1^2}{Ew_c^2}} \quad (10)$$

where L_c and w_c are the length and width of the coupling beam, respectively. The coupling beam are designed corresponds to a quarter wavelength of the center frequency to cancel the beam mass effect. Therefore, the equality given by Eq. (11) should be satisfied [13]:

$$(sin\,\alpha\,cosh\,\alpha+cos\,\alpha\,sinh\,\alpha)=0 \quad (11)$$

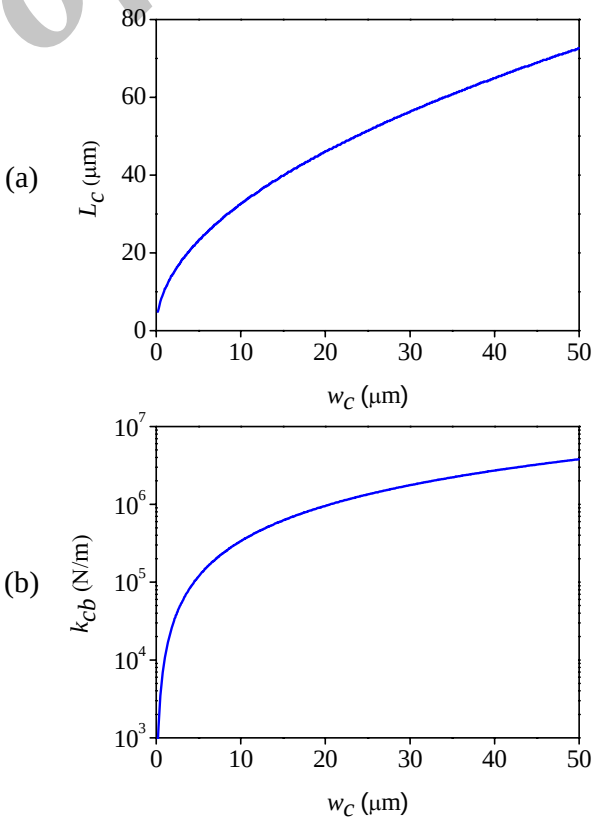

Fig. 3(a) The relationship between coupling beam length and beam width. (b) Analytically calculated coupling beam stiffness (k_{cb}) versus beam width.

As a result, Eqs. (10) and (11) can be solved to find the coupling beam length as shown in Fig. 3(a). It can be seen from the Fig. 3(b), as the coupling beam width decreases, the coupling beam stiffness decreases. However, the coupling beam width is limited by lithography, and it was chosen equal to 35 μm. Therefore, beam stiffness and beam length were obtained from Eqs. (11) and (9) as shown in Table 1.

Table 1 The design specifications of the ring filter.

Parameter	Explanation	Value	Unit
E	Young modulus	170	GPa
Y	Poisson ratio	0.31	-
P	Density	8900	kg/m^3
R_i	Inner radius	380	µm
R_o	Outer radius	590	µm
θ_e	Electrode angle	45	deg
L_s	Support beam length	93	µm
w_s	Support beam width	30	µm
L_c	Coupling beam length	61	µm
w_c	Coupling beam width	35	µm

3.2 Micromechanical Ring Resonator Design

According to Eqs. (7) and (8), with the given bandwidth of 30 kHz, center frequency of f_1=10.7 MHz and coupling beam stiffness of k_{cb}=2.223×10^6, resonator stiffness at the coupling location of (R_o, π/4) is obtained.

Micromechanical ring resonators can operate in their bulk-modes with different values of their inner and outer radii at a specific resonance frequency. For the given resonance frequency and mode shape, the relationship between the inner and outer radii of the ring resonator can be calculated via numerical solution of det($\mathbf{M}_{4\times4}$) = 0 as shown in Fig. 4(a). Therefore, the resonator stiffness for Extensional W.-Glass (EWG) mode is calculated using Eqs. (1) and (2). The side-support beams were attached to the quasi-nodal points of the EWG mode ring resonator, and were designed as the beams with sliding-fixed boundary conditions [12].

Therefore, these beams conform to vibrations of the ring resonator in flexural-mode with same resonance frequency as follows:

$$f = \frac{\pi\beta^2 w_s}{4\sqrt{3}L_s^2}\sqrt{\frac{E}{\rho}} \qquad (12)$$

where the subscript s denotes the support beam, and β=1.2498 denotes the flexural-mode constant. L_s and w_s are the length and width of the support beam, respectively.

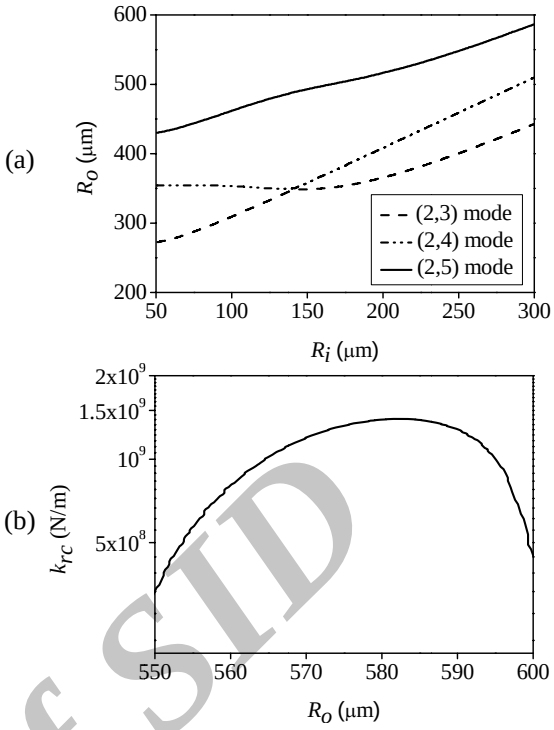

Fig. 4 (a) The relationship between the inner and outer radii in the ring resonator at f=10.7 MHz. (b) Resonator stiffness at (R_o, π/4) versus the outer radius for EWG mode.

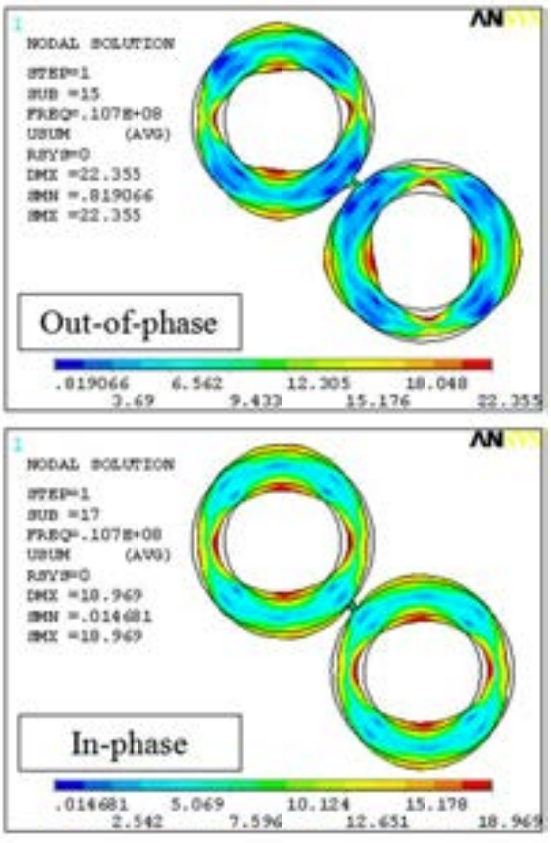

Fig. 5 ANSYS simulation for EWG ring filter with flexural-mode coupling beam.

Due to minimum feature size given by the Mylar mask in the fabrication process, the width of the support beams was set to 30 µm. The modal analysis of ANSYS software was used to verify the analytical derivations and design aspects of the ring filter. The mode shape simulations of out-of-phase and in-phase vibration EWG modes are shown in Fig. 5. As seen in Table 2, the analytical results agree well with ANSYS simulation. The EWG mode ring resonator has been presented recently by Bijari et al [17]. Fig. 6 shows the SEM of the fabricated ring resonator. The fabricated EWG resonator was able to operate with a high quality factor of 156170 using DC bias voltage of 90 V.

Table 2. Comparison between analytical resultsand ANSYS simulation.

Parameter	Analytical	ANSYS	Unit
Center frequency (f_1)	10.7	10.721	MHz
Band width (BW)	30	27.52	kHz
Resonator mass (M_r)	9.73×10^{-8}	2.29×10^{-7}	kg
Resonator stiffness (k_r)	4.4×10^{8}	1.03×10^{9}	N/m

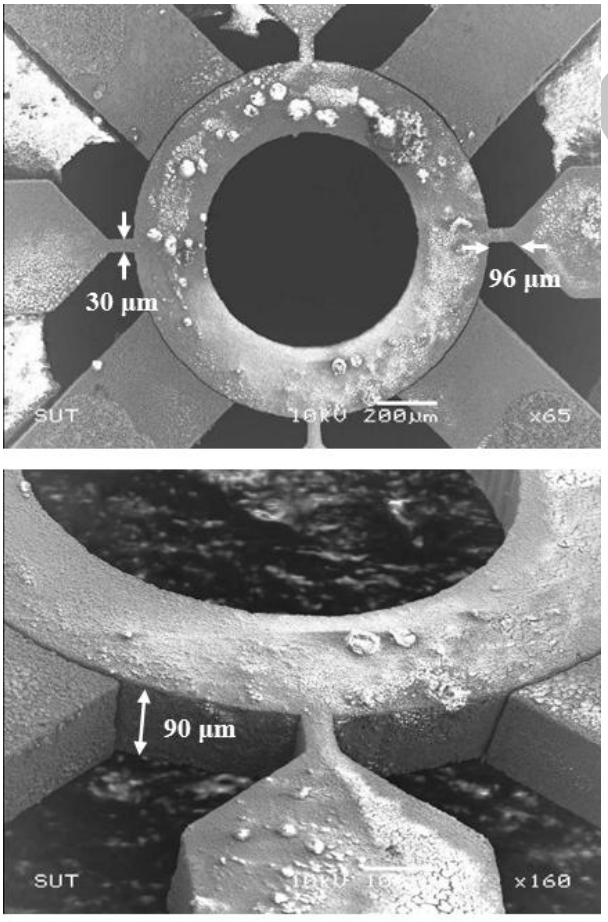

Fig. 6 SEM images of the micromechanical ring resonator.

3.3 Filter Termination

Due to the high Q of the EWG mode ring resonators, a micromechanical filter should be terminated with proper impedance values to reduce the ripple and provide a more flat pass-band. The required value of the total termination impedances for a filter with known center frequency and bandwidth is given by [6]:

$$R_{Qt} = R_m\left(\frac{BW}{f_1}\frac{Q_r}{q} - 1\right) = 2R_Q \qquad (13)$$

where R_m and Q_r are the motional resistance and quality factor of the constituent resonator, respectively, and q is a normalized parameter (q=1.414 for second-order Butterworth filter).

4 Fabrication Process

Micromechanical ring filter was fabricated using the fabrication process shown in Fig. 7. The proposed approach is based on the multi-step UV-lithography process and electroplating using nickel as a structural material. SU-8 photoresist was selected as a thick resist material to fabricate plating molds. Moreover, aluminum (Al) was used as sacrificial layer for realizing the capacitive gap between electrodes and resonators. The process begins with rigid graphite as the primary substrate and plating base. Before spin coating, a graphite substrate was cleaned by acetone under ultrasonic agitation. Graphite substrate coated with SU-8 was placed on the hot plate to reduce the internal stress.After cooling down to room temperature, the UV exposure could be performed using Mylar mask under UV light source with the exposure dosage of 600 mJ/cm^2. After UV exposure, the sample was post-baked and then cooled down to room temperature. The exposed SU-8 photoresist was developed using the SU-8 Developer at room temperature for 15 min. After the development, the substrate was rinsed with Isopropyl Alcohol (IPA) and oxygen plasma asher.

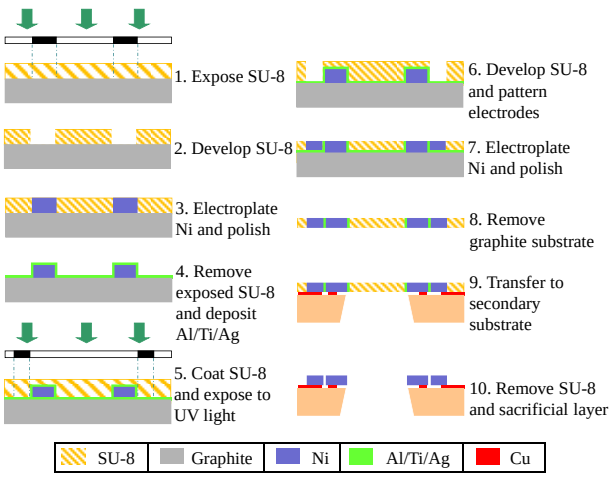

Fig. 7 Schematic representation of the ring filters fabrication process using UV-LIGA technology.

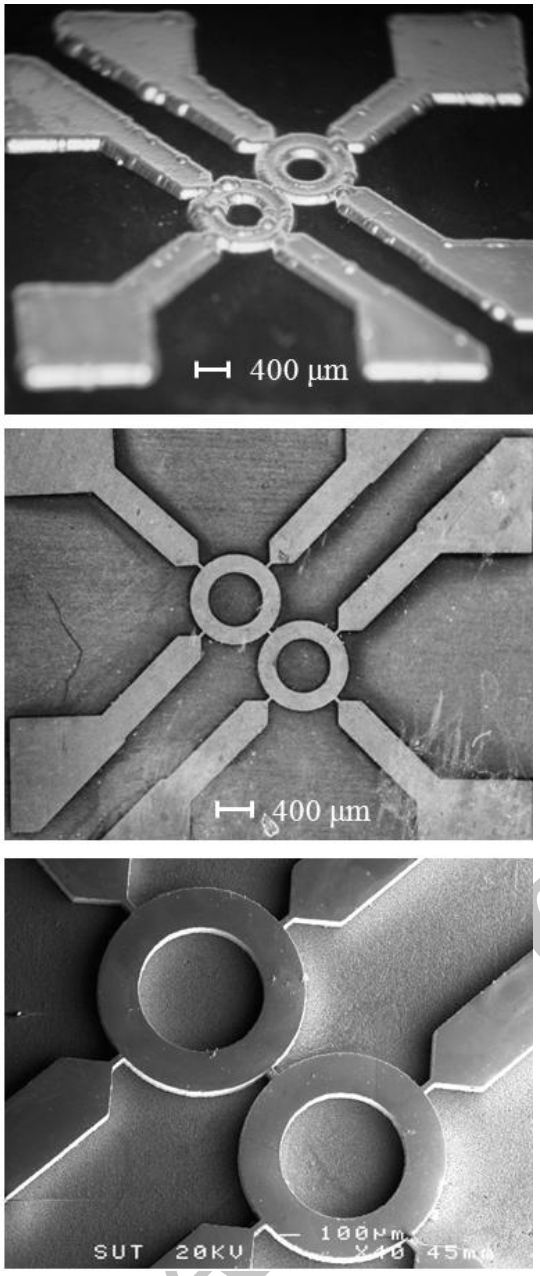

Fig. 8 The optical micrographs and SEM image of the main structure after (a) Nickel electroplating. (b) Surface polishing. (c) Removing the SU-8 photoresist.

Nickel electroplating was performed using a nickel sulfate plating bath and the current density was ramped from 5 to 30 mA/cm^2.

As shown in Fig. 8, the over plating parts were then mechanically leveled to the height of the photoresist by Polishing Device RotoPol-22 using the 5000 grit sandpapers. After nickel electroplating, the post exposure baked SU-8 photoresist was stripped with Remover PG (Microchem Inc.). This was followed by etching in a plasma asher with O_2/CF_4 gases to remove any remaining SU-8 photoresist from the surface.

4.1 Gap Fabrication Process

Aluminum (Al) was used as a sacrificial layer to define the electrode-to-resonator gap. Hence, after removing the electroplating mold, the structure was loaded into a DC sputtering system. The continuous sputtering time was limited to 2 min at 100 W DC power and sputtering was paused for 10 min before resuming another sputtering to prevent the high generated heat in the sputtering chamber. The sputtering cycle was repeated for 40 times to achieve high thickness of Al. Moreover, a tilted and rotated sputtering substrate was used to uniform deposition coating on the side walls of the ring structure. A thin film of titanium (Ti) was then deposited as an adhesive layer between the Al and a plating base layer of Ag. Next, the structure was coated by the SU-8 photoresist with the thickness of 200 µm. The SU-8 was patterned to define the electrodes with a UV light source with the expose dosage of 500 mJ/cm^2. As shown in Fig. 9, the Ni was then electroplated and the electrodes were leveled to the height of the main structure.

4.2 Transfer and Release Process

The sample was immersed into the nickel etchant TFG for 5 min to remove an eventual thin layer of Ni on the surface of capacitive gap.

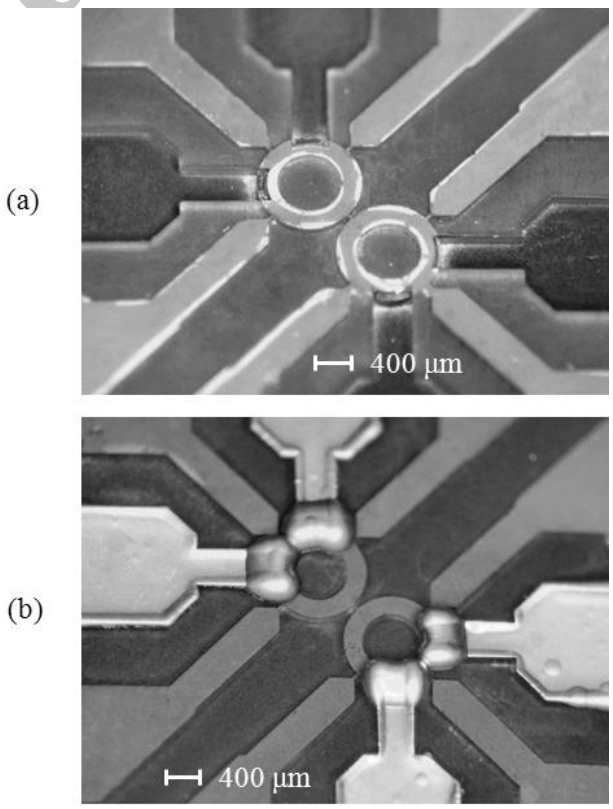

Fig. 9 The optical micrographs of fabrication process after (a) developing SU-8 to form the electrodes. (b) Ni electroplating.

To transfer the structure to secondary substrate, the surface of the sample was first covered by a thick layer of SU-8 photo-resist and a microscope glass slide was then attached on it. The sample was baked for 20 hours at 95 ˚C and next, the structure was released by mechanical polishing of graphite. The sample was again immersed into the nickel etchant TFG for 5 min. After that, sample was immersed in SU-8 Developer for 1 hrs to release the exposed SU-8 slab with filter structure, from the microscope glass slide. A patterned Printed Circuit Board (PCB) substrate with an embedded hole at its center was served as a secondary substrate. The exposed SU-8 slab with filter structure was transferred to the secondary substrate and the pads of the ring filter were connected to the substrate pads by conductive silver epoxy adhesive. The filter alignment to the new substrate was then checked under microscope. As shown in Fig. 10(b), to protect the pad connections against wet and plasma etching, the edges of the structure were buried with the SU-8 photo-resist and exposed to UV light. The suspended and released ring filter was achieved by etching in a plasma asher with O_2/CF_4 gases to remove the slab of exposed SU-8 photo-resist, and followed by wet etching the Al sacrificial layer.

To avoid the plasma etching of the protective SU-8 photo-resist on the pad connections, the sample was flipped over and plasma etching was performed through the hole in the back side of the substrate. Potassium hydroxide (KOH) solution (10%) was used to etch the sacrificial Al layer.

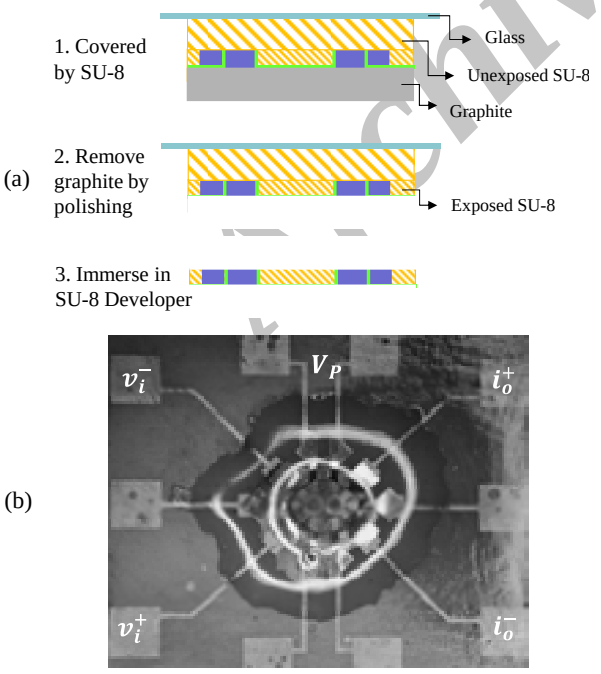

Fig. 10 (a) Schematic representations of the transfer process. (b) The photograph of the transferred structure on the secondary substrate.

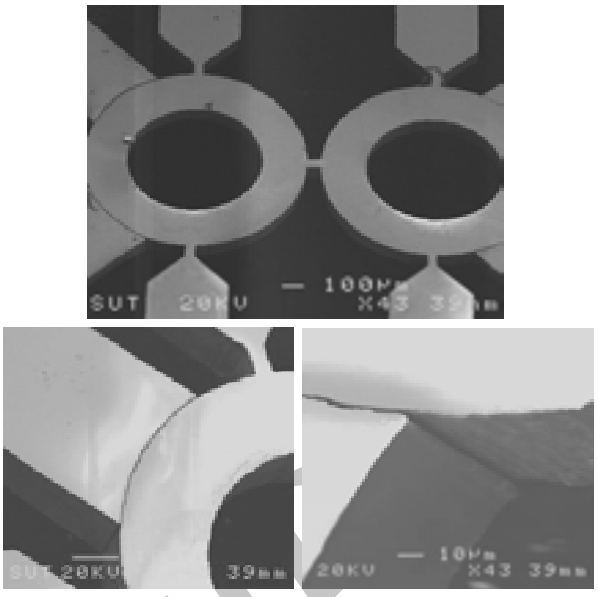

Fig. 11 SEM images of the released micromechanical filter.

5 Experimental Results and Discussion

The fabricated ring filter was characterized by a Scanning Electron Microscope (SEM). As shown in Fig. 11, the thickness and gap spacing of the filter are estimated about of 60 μm and 3μm, respectively.

5.1 Electrical Measurements

The fabricated ring filter was tested under vacuum in a two-port fully differential drive and sense configuration using a network analyzer. The filter was terminated by 8.2 MΩ resistors at the input and an output ports, the output voltage was amplified by a 20 dB gain voltage amplifier.

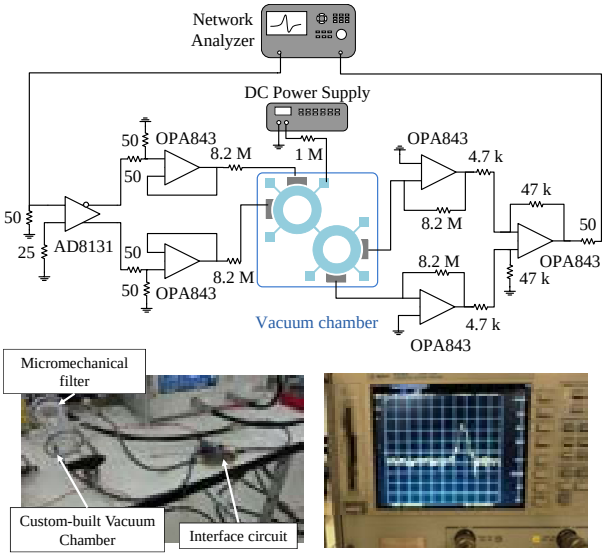

Fig. 12 The fully differential drive and sense setup for measurement of the micromechanical ring filter.

Fig. 12 shows a schematic view of the experimental setup. The interface circuit contains driving and sensing stages. The driving and sensing interface circuits were put outside a custom-built vacuum chamber equipped with DC and coaxial feedthroughs for connection to the fabricated ring filter placed in vacuum chamber. The custom-built vacuum chamber was evacuated down to 0.1 mbar and the DC-bias voltage was applied directly to the filter.

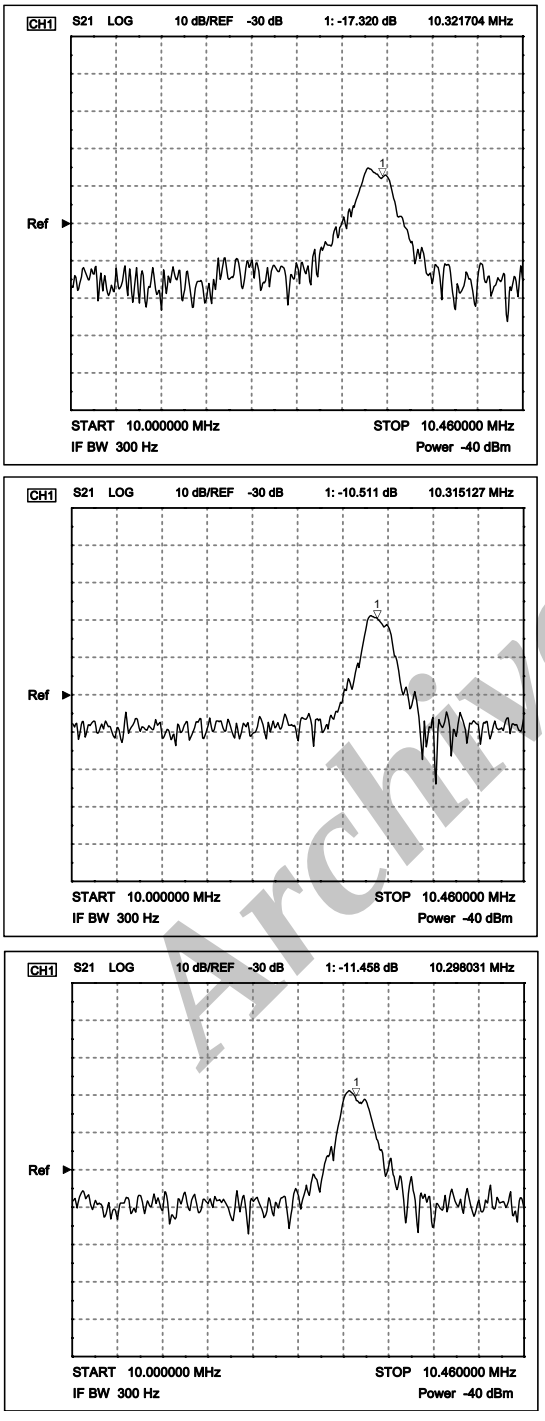

Fig. 13 Transmission (S21) plots of the fabricated ring filter over a frequency span of 460 kHz with IF bandwidth of 300 Hz and DC-bias voltage of (a) 30 V (b) 60 V (c) 90 V.

As shown in Fig. 13, the quality factor up to 351 for the EWG mode ring filter was experimentally derived from the transmission parameter, as the center frequency of 10.31 MHz over the 3dB bandwidth, for DC-bias voltage of 60 V. Moreover, the fabricated filter presents a percent bandwidth of 0.26 %, pass-band distortion of 3.8 dB, a stop-band rejection of 30 dB and a 20 dB shape factor of 2.48. The fabricated filter presents high insertion loss, which corresponds to the large motional resistance presenting in the micromechanical ring resonators. The shift between the measured bandwidth and center frequency with respect to the expected values can be attributed to the mismatches between constituent resonators, tolerance in position of the coupling beam, and Young modulus of nickel, which is a mechanical property related to the fabrication process, and changes from 131 to 202 GPa due to the condition of electroplating [18, 19].

6 Conclusion

In this paper, a novel low-cost fabrication process was developed in UV-LIGA technology to fabricate micromechanical ring filter. The design procedure was performed by a mechanical lumped element model. Micromechanical ring filter was successfully demonstrated with a high aspect ratio of 20 with gap spacing of 3 μm. Using rigid graphite as a primary substrate and SU-8 as an electroplating mold, micromechanical ring filter was fabricated with multi-step UV-lithography. The structure was released and transferred to the secondary substrate by new method. The fully differential drive and sense measurement setup was used to characterize the fabricated ring filter. The results show the center frequency of 10.31 MHz with a bandwidth of 26.3 kHz and stop-band rejection of 30dB using a DC-bias voltage of 60 V. Moreover, the fabricated filter presents a variation of a percent bandwidth between 0.25 to 0.33% with the applied bias voltage from 30 to 90 V. Based on the fabrication process, an optimized UV-LIGA can be used as a low-cost alternative to silicon-based micromachining processes.

Acknowledgment

The authors thank the students of SUT-MEMS laboratory including Chalermchai Pantong and Watcharapon Pummara and the staff of Synchrotron Light Research Institution (SLRI) (Thailand) for the use of X-ray from synchrotron radiation.

References

[1] Fathipour M., Refan M. H. and Ebrahimi S. M., "Design of a resonant suspended gate MOSFET with retrograde channel doping", *Iranian Journal of Electrical & Electronic Engineering*, Vol. 6, No. 2, pp. 77-83, Jun. 2010.

[2] Chandrahalim H., Bhave S. A., Polcawich R. G., Pulskamp J. S. and Judy D., "Fully-differential mechanically-coupled PZT-on-silicon filters", *Proceedings of IEEE International Ultrasonics Symposium Proceedings*, pp. 713–716, Beijing, China, Nov. 2008.

[3] Nguyen C. T.-C., "Micromechanical circuits for communication transceivers", *Proceedings of IEEE International Bipolar/BiCMOS Circuits and Technology Meeting*, Minneapolis USA, pp. 142-149, Sep. 2000.

[4] Wong A.-C., Clark J. R. and Nguyen C. T.-C., "Anneal-activated, tunable, 65MHz micromechanical filters", *The 10th International Conference on Solid-State Sensors and Actuators*, Sendai, Japan, pp. 1390- 1393, Jun. 1999.

[5] Bannon F. D., Clark J. R. and Nguyen C. T.-C., "High-Q HF microelectromechanical filters", *IEEE Journal of Sold-State Circuits*, Vol. 35, No. 4, pp. 512-526, Apr. 2000.

[6] Motiee M., Mansour R. R. and Khajepour A., "Novel MEMS filters for on-chip transceiver architecture, modeling and experiments", *Journal of Micromechanics and Microengineering*, Vol. 16, No. 2, pp. 407–418, Jan. 2006.

[7] Abdolvand R., Ho G. K. and Ayazi F., "Poly-wire-coupled single crystal silicon HARPSS micromechanical filters, Using Oxide Islands", *In Technical Digest Solid-State Sensors, Actuators*, pp. 242-245, South Carolina, USA, Jun. 2004.

[8] Wang S., Chandorkar S. A., Graham A. B., Messana M. W., Salvia J. and Kenny T. W., "Encapsulated mechanically coupled fully-differential breathe-mode ring filters with ultra-narrow bandwidth", *The 16th International Conference on Solid-State Sensors, Actuators and Microsystems*, Beijing, China, pp. 942-945, Jun. 2011.

[9] Basrour S., Majjad H., Coudevylle J. R. and Labachelerie M., "Simulation and characterization of high Q microresonators fabricated by UV-LIGA", *Technical Proceedings of International Conference on Modeling and Simulation of Microsystems*, South Carolina, USA, pp. 294-297, Jun. 2001.

[10] Huang W. L., Li S. S., Ren, Z. and Nguyen, C. T.-C., "UHF nickel micromechanical spoke-supported ring resonators", *The 14th International Conference on Solid-State Sensors and Actuators*, Lyon, France, pp. 323-326, Jun. 2007.

[11] Malek C. K. and Saile V., "Applications of LIGA technology to precision manufacturing of high-aspect-ratio micro-components and -systems: a review", *Microelectronics Journal*, Vol. 35, No. 2, pp. 131–143, Feb. 2004.

[12] Xie Y., Li S. S., Lin Y. W., Ren Z. and Nguyen C. T.-C., "1.52-GHz micromechanical extensional wine-glass mode ring resonators", *IEEE Transactions on Ultrasonics Ferroelectrics and Frequency Control*, Vol. 55, No. 4, pp. 890-907, Apr. 2008.

[13] Shalaby M. M., Abdelmoneum M. A. and Saitou K., "Design of spring coupling for high Q high frequency MEMS filters for wireless applications", *IEEE Trans. on Industrial Electronics*, Vol. 56, No. 4, pp. 1022-1030, Apr. 2009.

[14] Li S.-S., Demirci M. U., Lin Y.-W., Ren Z. and Nguyen C. T.-C., "Bridged micromechanical filters", *Proceedings of IEEE International Frequency Control Symposium and Exposition*, pp. 280-286, Aug. 2004.

[15] Bijari A., Keshmiri S. H. and Wanburee W., "Nonlinear modeling and investigating the nonlinear effects on frequency response of silicon bulk-mode ring resonator", *Iranian Journal of Electrical and Electronic Engineering*, Vol. 8, No. 1, pp. 45-54, Mar. 2012.

[16] Takano T., Hirata H., Tomikawa Y., "Analysis of non-axisymmetric vibration mode piezoelectric annular plate and its application to an ultrasonic motor", *IEEE Transactions on Ultrasonics Ferroelectrics and Frequency Control*, Vol. 37, No. 6, pp. 558-565, Nov. 1990.

[17] Bijari A., Keshmiri S.H., Leenaphet A., Wanburee W., Sriphung C. and Phatthanakun R., "A novel low-cost fabrication process for bulk-mode resonators in X-ray LIGA technology", *The 20th Iranian Conf. on Electrical Engineering (ICEE)*, Tehran, Iran, pp. 1-6, May. 2012.

[18] Cho H. S., Hemker K., Lian, K., Goettert J. and Dirras G., "Measured mechanical properties of LIGA Ni structures", *Journal of Sensors and Actuators A*, Vol. 103, No. 1, pp. 59-63, Jan. 2003.

[19] Zhou Z. M., Zhou Y., Yang C. S., Chen J. A., Ding G. F., Ding W., Wang M. J. and Zhang Y. M., "The evaluation of Young's modulus and residual stress of nickel films by microbridgetestings", *Journal of Measurement Science and Technology*, Vol. 15, No. 12, pp. 2389-2394, 2004.

Abolfazl Bijari was born in Birjand, Iran in 1982. He received B.S. degree in telecommunication engineering and M.S. in electronic engineering from Ferdowsi University of Mashhad (FUM), Iran in 2005 and 2007, respectively. He is currently PhD candidate in electronic engineering at the Department of Electrical Engineering, Faculty of Engineering, Ferdowsi University of Mashhad. His research interests include micromechanical resonators, filters and nonlinear effect on MEMS-based devices.

Sayyed-Hossein Keshmiri received his B.Sc. degree in Physics from Mashhad University in 1969, M. Tech. from Brunel University (London, UK) in 1971, and Ph.D. degree from The Pennsylvania State University (University Park, USA) in 1981. He started work in Ferdowsi University of Mashhad in 1971 first in Physics Department, and later was transferred to the Electrical Engineering Department. He is currently a professor of Electrical Engineering. His research interests include design and fabrication of photovoltaic solar cells, MEMS devices, transparent-conducting (TC) films, structural-defect passivation in silicon and in TC films, multilayer thin-film optical filters, and thin-film gas sensors.

Winai Wanburee was born in Roi-et, Thailand in 1982. He received the B.S. and M.S. degrees in the electrical engineering from Suranaree University of Technology (SUT), Nakhon Ratchasima, Thailandin 2005 and 2007, respectively. He has been with Synchrotron Light Research Institute (SLRI), Nakhonratchasima, Thailand as a member of Research Staff in SUT-MEMS Laboratory Since 2005. He is currently working toward the Ph.D. degree at Suranaree University of Technology since 2007. His research interests include design, analysis of micro-actuator and development of X-ray lithography process.

Chanwut Sriphung was born in Bangkok, Thailand, in 1973. He received the B.Sc. degree in computer technology from King Mongkut's University of Technology North Bangkok, the M.Sc. and M.Phil degree in Microsystems engineering from Heriot-Watt University, Edinburgh, UK. in 2006. He is currently a senior engineer working for Synchrotron Light Research Institute, Thailand. His main areas of interest focus on the micro-fabrication technology using UV and X-ray lithography for micro-parts, micro-sensors and micro-actuators.

Rungrueang Phatthanakun was born in Nakorn Ratchasima, Thailand, in 1981. He received the M.S. and P.h.D degrees in the electrical engineering from Suranaree University of Technology (SUT), Nakhon Ratchasima, Thailand in 2006 and 2010, respectively. He is currently a beamline scientist at the Beamline 6a: Deep X-ray Lithography (DXL), Synchrotron Light Research Institute, Thailand. His research interests include X-ray LIGA application, MEMS fabrication and simulation.